AGU ADVANCING EARTH AND SPACE SCIENCE

Earth and Space Science

RESEARCH ARTICLE
10.1029/2022EA002494

Is the Atlantic a Source for Decadal Predictability of Sea-Level Rise in Venice?

D. Zanchettin[1], S. Rubinetti[1,2], and A. Rubino[1]

[1]Department of Environmental Sciences, Informatics and Statistics, University Ca'Foscari of Venice, Mestre, Italy, [2]Now at Alfred Wegener Institute, Helmholtz Centre for Polar and Marine Research, List/Sylt, Germany

Key Points:

- The historical rate of sea-level rise in Venice contains large multidecadal fluctuations and interdecadal periods of near-zero trend
- Multidecadal sea-level trend variations in Venice follow those in the subpolar North Atlantic since the mid-20th Century
- Atlantic multidecadal variability paves the way for the exploration of decadal predictability of sea-level rise in Venice

Correspondence to:
D. Zanchettin,
davidoff@unive.it

Citation:
Zanchettin, D., Rubinetti, S., & Rubino, A. (2022). Is the Atlantic a source for decadal predictability of sea-level rise in Venice? *Earth and Space Science*, *9*, e2022EA002494. https://doi.org/10.1029/2022EA002494

Received 7 JUL 2022
Accepted 24 SEP 2022

Author Contributions:
Conceptualization: D. Zanchettin
Data curation: D. Zanchettin
Formal analysis: D. Zanchettin
Investigation: D. Zanchettin
Methodology: D. Zanchettin
Validation: D. Zanchettin
Writing – original draft: D. Zanchettin, S. Rubinetti, A. Rubino
Writing – review & editing: D. Zanchettin

Abstract Sea-level rise is one of the most critical consequences of global warming, with potentially vast impacts on coastal environments and societies. Sea-level changes are spatially and temporally heterogeneous on multiannual-to-multidecadal timescales. Here, we demonstrate that the observed rate of winter sea-level rise in the Italian city of Venice contains significant multidecadal fluctuations, including interdecadal periods of near-zero trend. Previous literature established a connection between the local sea-level trend in Venice and over the broad subpolar and eastern North Atlantic. We demonstrate that for multidecadal variations in sea-level trend such connection holds only since the mid-20th Century. Such multidecadal sea-level fluctuations relate to North Atlantic sea-surface temperature changes described by the Atlantic multidecadal variability, or AMV. The link is explained by combined effect of AMV-linked steric variations in the North Atlantic propagating in the Mediterranean Sea, and large-scale atmospheric circulation anomalies over the North Atlantic with a local effect on sea level in Venice. We discuss the implications of such variability for near-term predictability of winter sea-level changes in Venice. Combining available sea-level projections for Venice with a scenario of imminent AMV cooling yields a slowdown in the rate of sea-level rise in Venice, with the possibility of mean values remaining even roughly constant in the next two decades as AMV effects contrast the expected long-term sea-level rise. Acknowledging, understanding, and communicating this multidecadal variability in local sea-level rise is crucial for management and protection of this world-class historical site.

Plain Language Summary Environmental and socioeconomic impacts of sea-level rise are one of the major concerns of global warming. Here, we consider the case of the Italian city of Venice, one of the iconic locations for the potentially dramatic effects of sea-level rise. We show that the sea-level evolution in Venice during the past ∼150 years contains strong multidecadal fluctuations, so that periods of more than two decades when there is little or no trend occurred even in the recent past. We link these fluctuations with sea-level and climatic variations in the North Atlantic. In particular, we focus on the phenomenon known as Atlantic multidecadal variability, or AMV, which describes the alternation over multidecadal periods of warm and cold phases of the North Atlantic surface. Our results indicate that warm AMV phases are linked to faster sea-level rise in Venice and vice versa. Accordingly, we build sea-level rise scenarios for Venice until 2035 by considering an imminent AMV cooling as suggested by recent studies. The scenarios yield a temporary slowdown of sea-level rise as the AMV contrasts the effects of global warming. This sea-level variability can strongly impact on the management of protective measures against flooding currently operative in Venice.

1. Introduction

Increase in the average sea-level (SL) height is among the most dramatic implications of global warming, posing environmental, social and economic threats on coastal areas (Church et al., 2013; Oppenheimer et al., 2019; Thiéblemont et al., 2019). Recent estimates of rates of historical global-mean SL rise include, in the lower limit, 1.2 ± 0.2 mm/yr (90% confidence interval, period 1901–1990, Hay et al., 2015), 1.1 ± 0.3 mm/yr (99% confidence interval, period 1902–1990, Dangendorf et al., 2017) and 1.56 ± 0.33 mm/yr (90% confidence interval, period 1900–2018, Frederikse et al., 2020), with differences between estimates arguably arising from specificities on data set and period of analysis. The sixth assessment report of the Intergovernmental Panel on Climate Change (IPCC-AR6) indicates a historical global-mean SL rise of 20 ± 5 cm (best estimate and 5–95% range) in the period 1901–2018 (Fox-Kemper et al., 2021). In terms of impacts, it is the local SL change near the coast that matters, and observations demonstrate this to be strongly spatially heterogeneous over multiannual to multidecadal periods (e.g., Cazenave & Nerem, 2004; Chafik et al., 2019; Chambers et al., 2012; Kopp et al., 2014). This reflects the fact that global-mean SL trends and basin-scale and regional SL trends are caused by a different

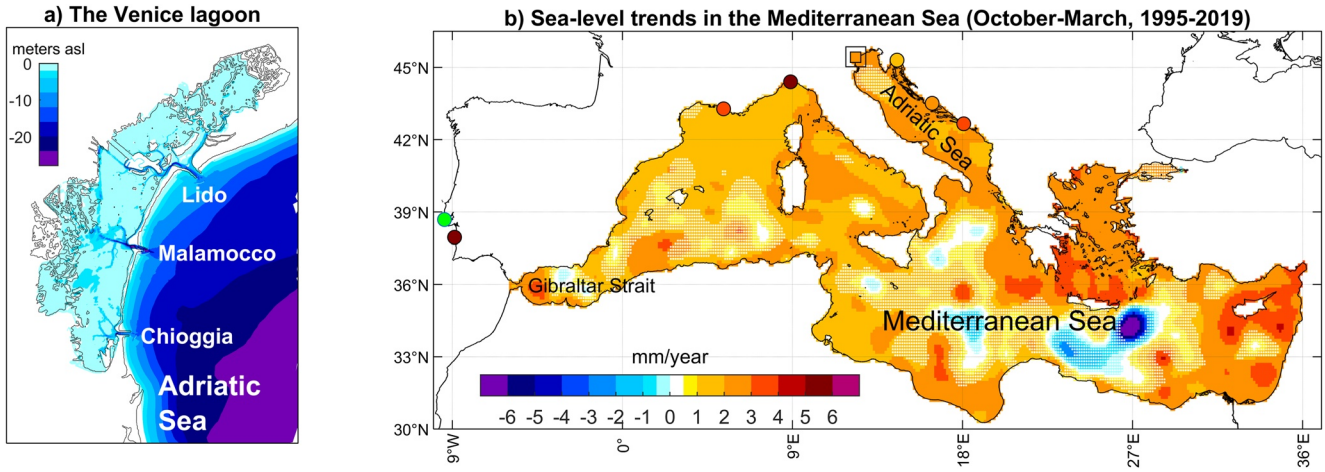

Figure 1. (a) Map of the Venice lagoon (redrawn from Zanchettin et al., 2021a; (b) map of the Mediterranean Sea with relevant locations for this study and winter (October–March average) SL anomaly trends in the Mediterranean Sea from satellite altimetry data over the period 1995–2019. White dots indicate where the trend calculated with a least squares linear regression model is not-significant according to the full-model *F*-statistics or the 95% confidence interval of the trend encompasses the zero value. The circles mark the location and winter SL trends of the PSMSL tide gauges considered in this study (from west to east: Cascais, Sines, Marseille, Genova/Genova2, Dubrovnik, Split, and Bakar); the green color indicates data unavailability over the considered period. The square marks the location and winter SL trend for the Venice tide gauge.

combination of processes, whose individual contribution can also vary through time (e.g., Camargo et al., 2021; Frederikse et al., 2020; Slangen et al., 2014, 2016).

The Italian city of Venice, built on pile in the central portion of the Venice Lagoon along the northern coast of the Adriatic Sea (Figure 1a), stands out among the coastal sites made iconic by the threat posed by SL changes and by the human efforts to mitigate it (Lionello, Barriopedro, et al., 2021). The historic town and the surrounding lagoon are included in the UNESCO list of World Heritage sites. Relative SL, that is, the local SL height relative to the local solid surface (Gregory et al., 2019; Rovere et al., 2016), has increased in Venice by about 35 cm during the past one-and-half century, partly due to land subsidence from natural as well as anthropogenic processes (e.g., Tosi et al., 2013; Zerbini et al., 2017) and partly to rise of the local mean SL due to climatic variations. There is agreement across studies that subsidence contributed to about half of the total relative SL observed in Venice in the course of the past one-and-half century (Zanchettin et al., 2021a). Accordingly, a recent estimate based on deseasoned tide gauge data, the long-term rate of Venetian SL rise corrected for subsidence is 1.23 ± 0.13 mm/yr for the period 1872–2019 (Zanchettin et al., 2021a, see Figure 2a).

The lowest part of the iconic San Marco square in the historical center of Venice is nowadays approximately 55 cm above the current average relative SL and astronomical tides have a local amplitude of about 50 cm; so, the lowest parts of the San Marco square can currently be flooded by a positive water height anomaly that is only a few centimeters above the astronomical high tide (Lionello, Barriopedro, et al., 2021). Indeed, temporary submersion of the city has been historically occurring during flooding episodes, which are events—widely known with their local name *acqua alta* (Battistin & Canestrelli, 2006; Ferrarin et al., 2021; Umgiesser et al., 2021)—when anomalous meteorological conditions phased with a favorable astronomical tide generate a storm surge in the lagoon (Lionello, Nicholls, et al., 2021). The increasing frequency of extreme surge events and the close succession of four peak water heights above 140 cm in autumn 2019 (baptized *acqua granda*, see, e.g., Cavaleri et al., 2020; Lionello, Nicholls, et al., 2021) revitalized the public concerns about the fate of Venice under continued SL rise and pushed on planned counteracting measures being put in use. A protective system made of mobile barriers at the lagoonal inlets to contrast the surges—the MoSE barriers—has already been operated for a few exceptional *acqua alta* events since October 2020, but it is not suitable for permanent closure (Lionello, Barriopedro, et al., 2021; Umgiesser, 2020).

In the assessment of future variations of local relative SL in Venice, current evaluations remain focused on projected changes during the 21st century under scenarios of increased anthropogenic greenhouse-gas emissions. Available estimates of long-term projected SL rise in Venice highlight, on the one hand, its strong dependency on global actions concerning greenhouse-gas emissions and the resulting temperature rise, and, on the

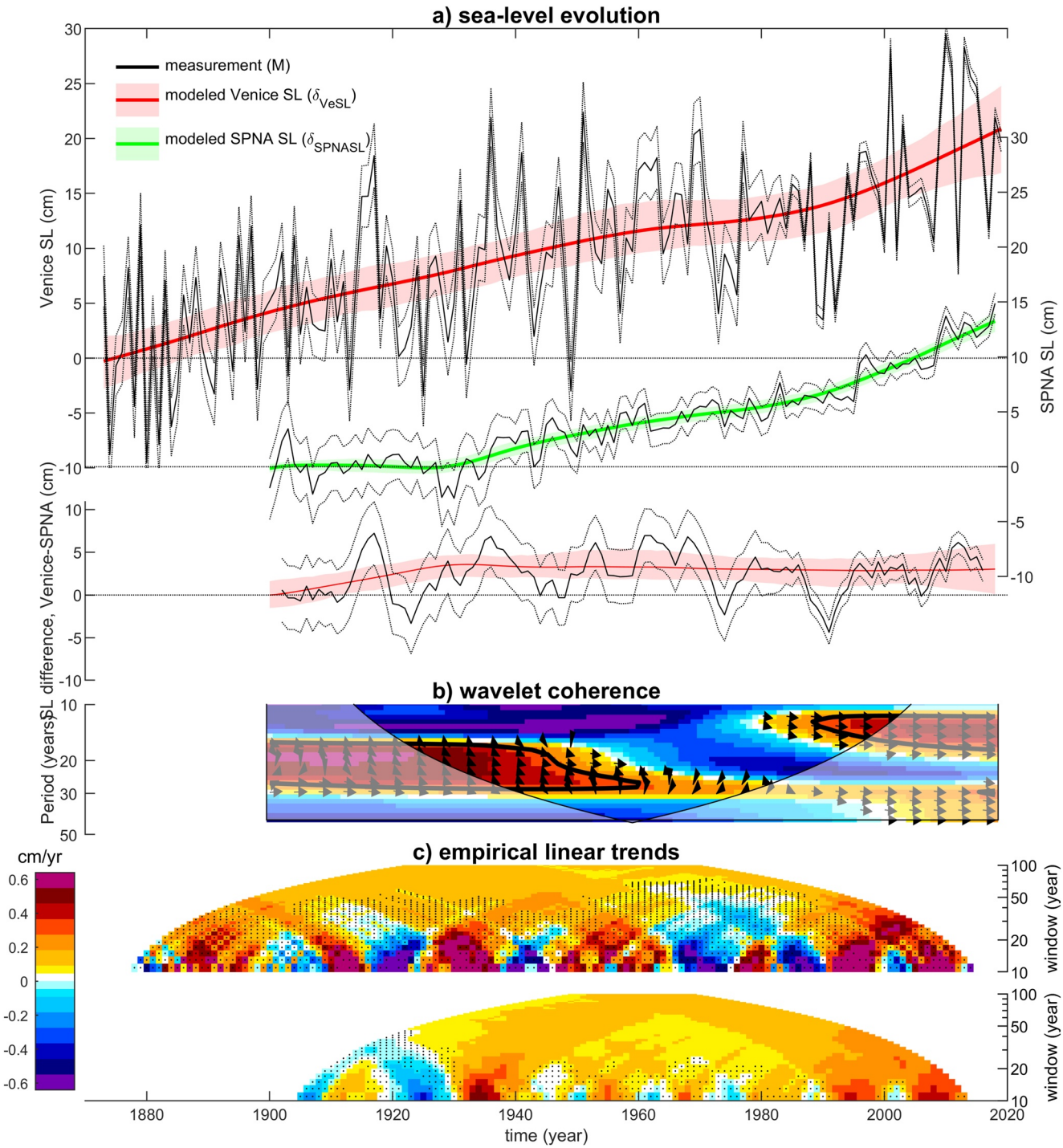

Figure 2. Comparison between historical sea-level (SL) evolution in Venice and in the Sub Polar North Atlantic. (a) Evolution of winter (October–March average) Venice SL (top) and annual Subpolar North Atlantic (SPNA) SL (middle), and their difference (bottom) shown in the form of measurements (M, black line, with associated uncertainty as dotted black lines, see methods) and modeled SL (δ, shading and colored lines). For the observed SL difference, time series are smoothed with a 5-year running average. Shading illustrates the 1st–99th percentile range for δ. (b) Wavelet coherence spectrum between M_{VeSL} and M_{SPNASL}. Thick contours individuate regions of the time-frequency space where the coherence is statistically significant at 95% confidence; arrows indicate the phase difference; the cone of influence is reported as a thin line and light shading. (c) Linear trends from M_{VeSL} and M_{SPNASL} estimated via least squares regression (*hac*, with order 0) for running windows of variable width along the observation period. The black dots indicate where the trend is not significantly different from zero, determined by the 95% confidence intervals of the regression coefficient encompassing the value of zero.

other hand, the existence of substantial uncertainties, where the sources of differences between estimates from different studies are choices on methods, models and assumptions to build the future scenarios of Venice SL, particularly related to background nonclimatic local SL variations linked to vertical land movement. Among available estimates, the very stringent RCP2.6 socioeconomic scenario yields a relative SL rise in Venice at 2100 of 47 cm (5–95 percentile range: 27–79 cm) with respect to the 1983–2001 reference period (Kopp et al., 2014), 60.3 ± 21.7 cm with respect to 2005 (Vecchio et al., 2019) and 47 cm (likely range 32–62 cm) with respect to the reference period 1986–2005 and excluding local atmospheric forcing (Zanchettin et al., 2021a). For the worst-case RCP8.5 socioeconomic scenario, estimates of SL rise in Venice at 2100 increase to 68 cm (5–95 percentile range: 41–107 cm, Kopp et al., 2014), 81.8 ± 25.8 cm (Vecchio et al., 2019) and 81 cm (likely range 58–110 cm, Zanchettin et al., 2021a), with higher values—up to 180 cm—not excluded under strong icesheet melting (Zanchettin et al., 2021a). These estimates represent the current state-of-the-art of projected SL rise for Venice used in the IPCC-AR6 by Working Group II for the box on Venice and its lagoon (Box 13.1 in Bednar-Friedl et al., 2022). Concerning the vertical land movement contribution to future relative SL rise in Venice, its assessment is complicated by the spatial heterogeneity of current subsidence rates observed at the lagoonal scale, with larger rates in the northern and southern portions compared to the central portion where Venice is located, as well as at the single-building scale (Tosi et al., 2018). Future subsidence-driven changes in the relative SL on a century-scale are thus difficult to quantify, also due to the unpredictable local anthropogenic component, and proposed estimates span from 0.72 ± 0.33 mm/yr (Kopp et al., 2014) to 1 mm/yr (Zanchettin et al., 2021a) and 3.3 ± 0.85 mm/yr (Vecchio et al., 2019).

In terms of impacts on the city of Venice, an increase of about 55 cm from the current mean relative SL (close to the central estimate for SL rise at the end of the century under weak anthropogenic greenhouse-gas emission scenarios) would reach the elevation of parts of the San Marco square, which would then be submerged daily by astronomical tides alone, whereas an increase of about 80 cm (close to the central estimate for SL rise at the end of the century under strong anthropogenic greenhouse gas emission scenarios) or 120 cm would extend the issue of almost permanent submersion to about 12% and more than 70% of the city, respectively. The projected SL rise will also be the main driver of increasing extreme water heights and increasing flood potential in Venice, posing a challenge to the operability of MoSE barriers against *acqua alta* events as close as within a few decades from now in the worst-case scenario (Lionello, Barriopedro, et al., 2021).

Besides long-term future scenarios that focus on the expected climate response to external forcings, near-term predictions remain an important yet neglected topic. Near-term SL predictions aim at the quantification of the range of possible SL evolutions within the next couple of decades or so accounting for the effect of both, external forcings and initial climate conditions. Viability and need for near-term predictions of Venice SL stems from the multidecadal variations detected in the rate of Venetian mean SL rise including periods of negative trends (Zanchettin et al., 2021a) . The search of large-scale climatic precursors of Venice SL variability must account for the fact that it closely depends on SL variations in the Adriatic Sea and, in turn, in the Mediterranean Sea (e.g., Bruni et al., 2022; Zanchettin et al., 2021a). Accordingly, it is well established that the North Atlantic climate affects Adriatic SL and, hence, Venice SL trends and variability on interannual-to-decadal timescales through atmospheric teleconnections, in particular linked with the large-scale mode of atmospheric circulation variability known as North Atlantic Oscillation or NAO (e.g., Galassi & Spada, 2014; Zanchettin et al., 2006, 2009, 2021a; Meli & Romagnoli, 2022). Then, basin-wide Mediterranean SL variations are associated on a broad range of timescales with analog SL variations in the eastern boundary of the North Atlantic ocean through water mass exchanges at the Strait of Gibraltar (e.g., Lionello, Barriopedro, et al., 2021, see Figure 1b). Accordingly, a tight connection has been identified between 20th century SL evolution in Venice and in the subpolar and eastern North Atlantic (Lionello, Barriopedro, et al., 2021; Zanchettin et al., 2021a), the latter being a region known to feature prominent predictable multidecadal oceanic variability (e.g., Latif et al., 2022; Smith et al., 2020). Multidecadal North Atlantic ocean variability is often described through basin-scale sea-surface temperature (SST) anomalies and referred to as Atlantic multidecadal variability or AMV (Enfield et al., 2001; Mann et al., 2020; Zanchettin et al., 2021a), whose index has been shown to covary with the Venice SL record (Scafetta, 2014). After a warm phase established in the late 1990s and persisting to the present, the AMV may undergo a sustained negative phase according to some recent studies (Frajka-Williams et al., 2017; Omrani et al., 2022), which may then significantly affect Venice SL trends in the next decades.

In this paper, we quantify temporal variations in the rate of SL rise in Venice, put them in the context of SL variability along the Mediterranean coasts and link them with SL variability and climatic phenomena in the North Atlantic sector, specifically with multidecadal fluctuations in North Atlantic SST and associated steric SL variations and large-scale atmospheric anomalies. We outline possible implications of a temporary North Atlantic surface cooling in the upcoming decades for the near-term predictability of SL rise in Venice.

2. Data and Methods

2.1. Historical Data

The time series of Venice SL (VeSL) data are the seasonal-average tide gauge data described in Zanchettin et al. (2021a) and available as "VLMcorrectedRSL" in Zanchettin et al. (2021b). These data were obtained by removing the contribution of local subsidence from the historical tide gauge data using the vertical land movement estimate for Venice provided by Zerbini et al. (2017). The subsidence curve was obtained empirically by interpolating the heights of various benchmarks including leveling data close to the Punta della Salute tide gauge, Global Positioning System and Synthetic Aperture Radar interferometry measurements (Zerbini et al., 2017). Therefore, the VLMcorrectedRSL time series is not a direct measurement of the Venice SL, but an indirect evidence of it obtained by a linear combination of tide gauge data and a subsidence model.

Average values for the winter semester (October–March) are obtained by averaging the seasonal estimates for October–December and January–March provided in Zanchettin et al. (2021b). Using the winter semester allows to encompass the period of the year when storm surges typically occur in Venice (e.g., Lionello, Nicholls, et al., 2021). The original time series provided by Zanchettin et al. (2021b) were not associated with an uncertainty estimate. Here, we use the raw tide gauge data provided by Battistin and Canestrelli (2006) and by the "Centro Previsioni e Segnalazioni Maree of the Venice Municipality" (data available at the url: https://www.comune.venezia.it/node/6214, last accessed on 21 June 2022) to calculate the yearly standard error of the mean for the October–December and January–March seasonal averages. Then, these two seasonal uncertainty estimates are linearly combined to produce an October–March uncertainty (see Section 2.2). The time series of winter Venice SL and associated uncertainty is illustrated in Figures 2a and available as Zanchettin (2022).

A long SL time series is also available for Trieste, about 150 km to the east of Venice along the northeastern Adriatic coast. The Trieste time series is neglected in this study as it is strongly affected by missing data in the nineteenth century. SL trend estimates from Trieste and Venice (VLMcorrectedRSL) time series are known to be largely consistent over a broad band of timescales, supportive of a rather uniform SL trend in the northern Adriatic (Zanchettin et al., 2021a).

An analysis of coastal SL variations from several tide gauges along the Mediterranean and eastern North Atlantic coast is performed to support the physical interpretation of the Venice SL variability and to illustrate the potential of the proposed approach for broader SL variability beyond the specific case of Venice. To this purpose, monthly mean tide gauge data are acquired through the Permanent Service for Mean Sea Level, available at the url: www.psmsl.org (Holgate et al., 2013; Permanent Service for Mean Sea Level et al., 2022). The location of the considered tide gauges is shown by the circles in Figure 1b. The considered tide gauges within the Mediterranean Sea pertain to areas (the Western basin and the Adriatic Sea) where SL trends from tide gauge and from satellite altimetry data show the best agreement according to a recent assessment (Bruni et al., 2022).

Monthly average data of SL anomaly (defined as the sea-surface height above the mean sea-surface referenced to the period 1993–2012) in the Mediterranean Sea from altimetry measurements is obtained from the Copernicus Climate Change Service (C3S, http://climate.copernicus.eu), product version 2019. The reference mission used for the altimeter intercalibration processing is Topex/Poseidon between 1 January 1993 and 23 April 2002, Jason-1 between 24 April 2002 and 18 October 2008, OSTM/Jason-2 between 19 October 2008 and 25 June 2016, Jason-3 since 25 June 2016. Consistency between trend estimates from tide gauge and satellite altimetry data varies in the different subbasins of the Mediterranean Sea, with overall good agreement in the Adriatic Sea (Bruni et al., 2022).

Subbasin scale average SL for the North Atlantic is provided by Frederikse et al. (2020). Specifically, we use the data referred to as "Subpolar North Atlantic" (SPNA), which encompasses the subpolar North Atlantic, the

eastern North Atlantic, the Arctic, and the Mediterranean Sea. Frederikse et al. (2020) also provide estimates of contributions to SL changes of ice-mass loss, terrestrial water storage, and thermal expansion of the ocean.

We use the unsmoothed 1856-present monthly time series of the Atlantic Multidecadal Oscillation index calculated at NOAA PSL based on the Kaplan SST data set, available at the url: https://psl.noaa.gov/data/timeseries/AMO/.

Gridded SST observational data for the period 1870–2019 are obtained from the Hadley Center Sea Ice and Sea-Surface Temperature data set (HadISST1, Rayner et al., 2003).

The North Atlantic Oscillation (NAO) index is the updated monthly time series provided by Jones et al. (1997), available at the url: https://crudata.uea.ac.uk/cru/data/nao/

Reanalysis data are from the monthly NOAA-CIRES 20th Century Reanalysis V2 data set (Compo et al., 2011). Support for the 20th Century Reanalysis Project data set is provided by the U.S. Department of Energy, Office of Science Innovative and Novel Computational Impact on Theory and Experiment (DOE INCITE) program, and Office of Biological and Environmental Research (BER), and by the National Oceanic and Atmospheric Administration Climate Program Office.

2.2. Time Series Analysis

Least square linear regressions are performed using the Matlab function *regress*. The function *hac* is used to calculate SL trends and associated uncertainties for Venice and the SPNA. HAC estimators are designed to correct for the bias in the ordinary least squares standard error calculation introduced by autocorrelation, and so provide a more robust setting for inference regarding the significance of regression coefficients. HAC estimators are sensitive to the application of a prewhitening filter (Andrews & Monohan, 1992) and we provide estimates for the order of the vector autoregression model (below order 10) that locally maximizes the standard error.

The local subsidence estimate for Venice was not provided with an uncertainty estimate, which affects the calculation of uncertainty of trends for the "VLMcorrectedRSL" time series. Uncertainty in the trend estimate for the Venice SL (Δ_{VeSL}) is therefore calculated via linear propagation of uncertainties in trend estimates for the original tide gauge data (Δ_{VeTG}) and the subsidence components (Δ_{VLM}), calculated according to the equation $\Delta_{\mathrm{VeSL}}{}^2 = \Delta_{\mathrm{VeTG}}{}^2 + \Delta_{\mathrm{VLM}}{}^2$. The same approach for propagation of uncertainty is applied to other combined quantities.

Statistical significance for differences between data subsets obtained by composite analysis is performed using the Mann-Whitney *U* test.

Wavelet coherence spectra are calculated using the cross wavelet and wavelet coherence package by Aslak Grinsted, John Moore, and Svetlana Jevrejeva available at the url: https://github.com/grinsted/wavelet-coherence (Grinsted et al., 2004; see also: Torrence & Webster, 1999).

2.3. Statistical Model for Stochastic Trends

We apply a statistical model developed under the Bayesian hierarchical framework to separate uncertainties embedded in the SL time series at the data level (e.g., associated to the instrumental noisy observations), at the process level (i.e., the SL trend, which is not directly observable) and at the models' parameter level. Tebaldi et al. (2005), Buser et al. (2009), Duan and Phillips et al. (2010), Kang et al. (2012), and Arisido et al. (2017) provide examples of the application of Bayesian statistics in the field of climate research, and we only focus here on a few general concepts regarding our specific application. Bayes' theorem is used to estimate the unknowns (i.e., hidden process and model parameters) with associated uncertainty through the calculation of their posterior distribution conditioned to available observations (i.e., the data). This approach allows to surpass limitations related to the explicit treatment of uncertainties required by empirical approaches, in this case especially relevant to the subsidence estimate for the Venice SL. In practice, we assume that all uncertainties arising from preprocessing of the Venice SL data remain embedded in the "VLMcorrectedRSL" time series.

Table 1
Relevant Settings for the DLM Applied to Time Series of Selected Variables

	Venice SL (VeSL)	SPNA SL (SPNASL)	AMV (AMV)	wmNA SST (wmNASST)	emNA SST (emNASST)
Initial state δ(0),β(0)	0,0.2	0,0	0.018,0	10.6,0	17.6,0
Initial state uncertainty covariance	[2.4, 0; 0, 0.1]	[5.6, 0; 0, 0.01]	[0.15 0; 0 0.21]	[0.74 0; 0 0.11]	[0.31 0; 0 0.03]
τ_M	1	$0.5 \cdot (\mathrm{SPNASL}_{\mathrm{upper}} - \mathrm{SPNASL}_{\mathrm{lower}})$	0.1	0.1	0.1
Threshold for β	0.0025	6.25e−4	0.001	0.001	0.001
Sampled realizations	658	899	800	999	999

Note. SPNAupper and SPNAlower are upper and lower estimates of SPNA SL provided by Frederikse et al. (2020). Threshold for β is the threshold variance of β realizations to be exceeded to retain the sampled parameters.

The statistical model is the same developed by Laine et al. (2014) within the dynamic linear model (DLM) framework based on a state-space approach. According to the DLM framework, unobservable state variables are used that allow direct modeling of the hidden process generating the measured data. Specifically, the state δ at discretized time t (in this case corresponding to a certain year in the time series) is observed through the associated measurement M via the data model:

$$M_J(t) = \delta(t) + \varepsilon_M(t) \tag{1}$$

where ε_M is a Gaussian white noise with zero mean and variance $\tau^2{}_M$ (see Table 1). ε_M contains observational errors but also includes higher frequency variations with respect to the SL trend, which is the process of interest, such as interannual variability. In the process model, δ evolves through time according to the local stochastic trend β as follows:

$$\delta(t) = \delta(t-1) + \beta(t-1) + \varepsilon_\delta(t) \tag{2}$$

where $(t-1)$ indicates the previous sample (in this case corresponding to the year before year t), ε_δ is uncorrelated Gaussian white noise with zero mean and variance T_δ^2. The effect of ε_δ is to allow the level to rise and fall. Dynamics of β are described as a random walk:

$$\beta(t) = \beta(t-1) + \varepsilon_\beta(t) \tag{3}$$

The system of Equations 1–3 corresponds to the system of Equations 3–5 in Laine et al. (2014).

The larger the variances of the Gaussian noises, the greater the stochastic movements in the level and changes in the stochastic slope. If $\tau_\delta^2 = \tau_\beta^2 = 0$, the local stochastic trend collapses to a linear deterministic trend.

The DLM uses the *dlmsmo* Matlab function developed by M.J. Laine and available at https://github.com/mjlaine/dlm.

The posterior distribution on the left term of Bayes' theorem is sampled through a Markov Chain Monte Carlo method, in this study based on a slice-sampler algorithm (Radford, 2003). Then, Kalman filter and Kalman smoother are used to iteratively sample the states of the process along a Monte Carlo Markov Chain to sample from the marginal distributions for each of the state components (see Laine et al., 2014, for details). In the Bayesian framework, specification of the prior distribution for the unknown parameters (in this case: τ_M^2, τ_δ^2, τ_β^2) is required. We define weakly informative lognormal (LN) priors in the form LN(0,1) for all parameters. Only parameter sets sampled along the Monte Carlo chain yielding a realization of β with variance exceeding a threshold value are retained (see Table 1), so that realizations describing a linear trend—corresponding to constant β values through time—are not sampled. The DLM is applied to time series of selected variables using the settings provided in Table 1. Estimates of the various components of the DLM for each considered variable are indicated by adding the variable's name as subscript to the component (e.g., β_{VeSL}).

2.4. SL Scenarios

Future scenarios of AMV evolution between 2020 and 2035 are generated based on values of the cumulative distribution function for the Normal distribution evaluated at 0.25 intervals between −2 and 3.25. This reference evolu-

tion is scaled by the expected change toward negative/neutral AMV values (0.2 for the "relaxation scenario" and 0.4 for the "fluctuation scenario", see Section 4.2 and then subtracted from the average of the last value of δ_{AMV} in each of the 800 sampled realizations of the process. The so-obtained AMV scenario data are used as predictors for linear regression models to obtain historical and scenario realizations of β_{VeSL} conditioned to the AMV.

These realizations of AMV-induced SL changes are combined with probabilistic scenarios of Venice SL that describe the expected Venice SL responses to global climate changes induced by anthropogenic greenhouse gas forcing under different emission assumptions (Thieblemont et al., 2019; Zanchettin et al., 2021a, 2021b).

3. Results

3.1. Sea-Level Trend From Least Squares Regression

Figure 1b illustrates winter Mediterranean SL trends for the period 1995–2019 obtained from satellite altimetry data and tide gauges with ordinary least squares linear regression. The results agree with SL trends obtained by Zanchettin et al. (2021a) using data from a different altimetry product (ESA SLCCI V2) and over a different period, where spatially heterogeneous trends reflect ocean circulation effects on local SL variability. Accordingly, altimeter data indicate nonsignificant winter SL trends over extensive regions across all Mediterranean subbasins, including portions of the northern Adriatic. Tide gauge data tend to have larger winter SL trends compared to satellite-based estimates, which may reflect both, inclusion of subsidence in the former and limitations of the latter for coastal regions. The agreement between winter SL trends from altimeter data and tide gauges improves in the northern Adriatic, including Venice for which subsidence is removed in the VLMcorrectedRSL time series.

Figure 2a illustrates the historical evolution of winter Venice SL (M_{VeSL}) and SPNA SL (M_{SPNASL}). Based on data for the common period 1900–2018, the linear trend estimated with least squares regression for M_{VeSL} is 1.18 mm/yr ([0.60 1.76] as ±2 standard error range including standard error estimates using *hac*, order 5, and by propagating uncertainties in trends of relative SL and subsidence, see Section 2) with R^2 0.348. The linear trend for M_{SPNASL} is 1.08 mm/yr ([0.66 1.50], with *hac*, order 1) with R^2 0.844. The much larger R^2 value obtained for the SPNA SL compared to the Venice SL record indicates that in the latter the long-term linear trend is a less important and less certain component of the total variability, likely due to the presence of strong variations in the broad band encompassing interannual-to-interdecadal timescales. Linear trend estimates for Venice and SPNA SL overlap with each other within uncertainties but the best estimate of the trend for Venice is overall slightly larger than for the SPNA, which is also seen as the predominantly positive SL differences ($M_{VeSL} - M_{SPNASL}$) illustrated at the bottom of Figure 2a.

The wavelet coherence spectrum in Figure 2b further illustrates the variable connection between decadal and multidecadal variations in M_{VeSL} and M_{SPNASL}. There is a significant tight cophase at decadal timescales between both time series in the most recent decades (since around 1980), associated with a consistent stronger SL rise compared to the preceding period. Conversely, the earlier part of the 20th century is characterized by common strong but phase-lagged interdecadal variability around periods of 20–30 years, where Venice SL appears to lead SPNA SL variations by a few years. This specifically appears to be related with the transition around 1930 from a weaker to a stronger SL rise in M_{SPNASL}. Linear trends over moving windows of variable width in Figure 2c illustrate the effects of the strong interannual-to-interdecadal variability contained in M_{VeSL}: interdecadal periods—up to almost half century—of evanescent trends, that is, statistically not different from zero (see black dots in Figure 2c), are found also in the second half of the 20th century, especially during the 1960s, 1970s, and 1980s. By contrast, the corresponding persistently positive trend estimates for M_{SPNASL} indicate an ongoing SL rise during these decades, although with a temporary weaker rate. The dominance of interannual variability in M_{VeSL} can be further highlighted by its connections with patterns of surface ocean and atmospheric variability in the North Atlantic and Euro-Mediterranean sectors. The regression pattern of detrended SST on detrended M_{VeSL} highlights the eastern Mediterranean Sea, particularly in the Adriatic and Levantine basins, and reveals a quadrupole pattern that superposes well on the inverse regression pattern of detrended SST on the NAO (Figures 3a and 3d). Composite analysis of atmospheric circulation anomalies around M_{VeSL} reveals that anomalously high Venice SL is linked with an extensive negative pressure anomaly centered over the Bay of Biscay and reaching the midlatitude eastern North Atlantic, the British Isles and the Euro-Mediterranean region (Figure 4a). Over the Adriatic basin, this is associated with a SL rise due to the inverse barometer effect. The near-surface wind composite includes an anomalous southwesterly flow over the Ionian and Adriatic Seas, whose meridional component

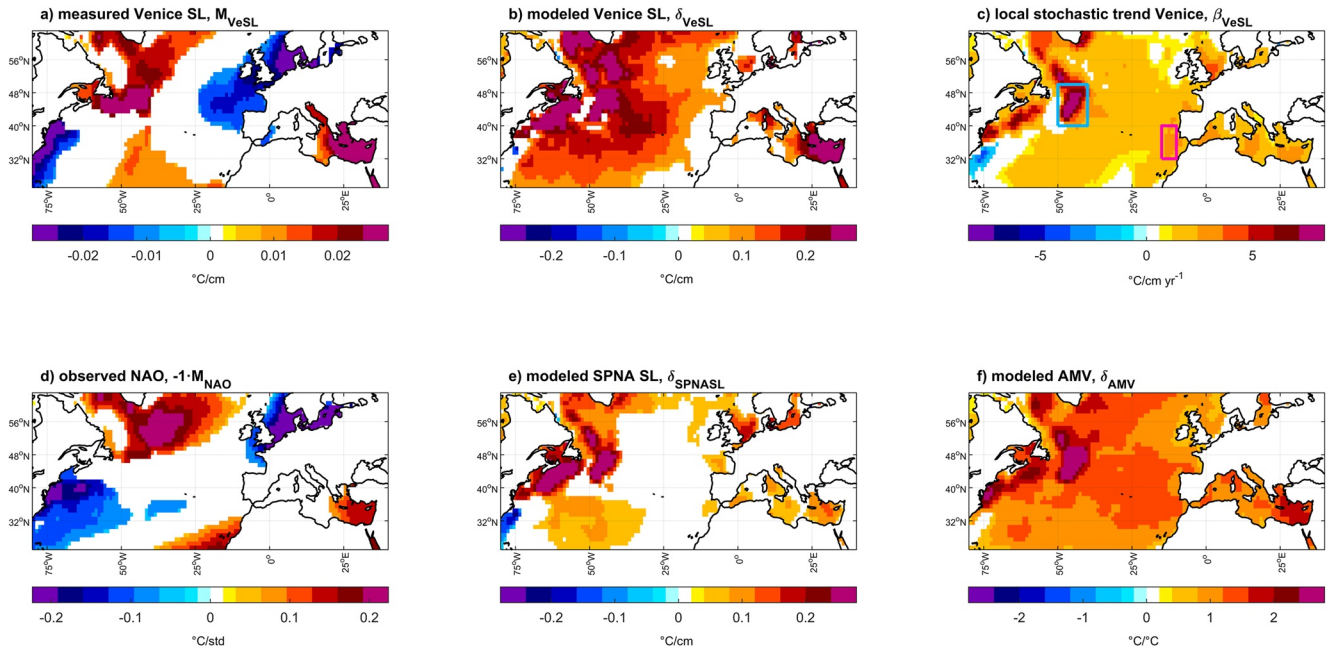

Figure 3. Regression patterns of North Atlantic and Mediterranean sea-surface temperature (SST) on selected indicators of climatic variability linked with Venice sea-level (SL) change, including (a) measured Venice SL, (b) modeled Venice SL (δ_{VeSL}) and (c) associated local stochastic trend β_{VeSL}, (d) the North Atlantic Oscillation (NAO), (e) modeled Sub Polar North Atlantic (SPNA) SL (δ_{SPNASL}), and (f) the modeled Atlantic multidecadal variability (AMV). All data refer to averages over the winter (October–March) semester, linearly detrended before analysis. Regressions are shown only for local SST where the linear regression model is statistically significant at $p < 0.05$. Boxes in panel (c) illustrate the regions referred to as western midlatitude North Atlantic (wmNA, magenta) and eastern midlatitude North Atlantic (emNA, turquoise).

thus contributes to piling up of waters toward the northern Adriatic as observed during the Sirocco wind circulation (e.g., Zanchettin et al., 2021a). Furthermore, the atmospheric circulation anomaly includes an anomalous westerly flow over the subtropical North Atlantic, which contributes to pushing Atlantic waters toward Gibraltar and further from the Western toward the Eastern Mediterranean. The anomalous circulation pattern agrees with earlier analyses for the Mediterranean region and a different data set (Zanchettin et al., 2021a) that were used to corroborate the link between interannual-to-decadal winter variability of NAO and Venice SL. The present analysis over a more extensive domain encompassing the North Atlantic, European and Mediterranean regions confirms that the atmospheric circulation anomaly associated with high Venice SL superposes well on the NAO pattern, concerning the location of the anomalous pressure centers (Figure 4a) and the overall structure of the pattern (weighted R^2 between Venice SL and NAO 1,000 hPa geopotential height patterns is 0.80 with weighted root mean squared error of 32 m).

Overall, least squares regression trend estimates thus suggest that Venice SL and SPNA SL are not as robustly and tightly linked as previously suggested. However, discrepancies might be linked to the substantial interannual-to-decadal variability contained in both historical records. This variability, for Venice SL, is especially strong and traces back to NAO-related atmospheric dynamics.

3.2. Sea-Level Trend From DLM

We use the dynamic linear model (1–3) to separate the SL trend from the observational noise and the strong interannual-to-decadal variability that especially affects the Venice SL time series. The modeled SL (δ) and the underlying local stochastic trends (β) for Venice and SPNA SL are illustrated in Figures 2a and 5a, respectively. Differences between δ_{VeSL} and δ_{SPNASL} are also illustrated in Figure 2a. The full-period average of β_{VeSL} is 1.46 mm/yr ([1.25, 1.69] as 5–95 percentile range), consistent within uncertainties with previous estimates (Zanchettin et al., 2021a; Zerbini et al., 2017; see also Figure 5a, circles and bars on the right). The R^2 statistics measuring the fraction of variance of M_{VeSL} explained by ranges between 0.465 and 0.491 (5–95 percentile range) for the individual realizations of δ_{VeSL} (average across realizations is 0.486). These values compare well with the

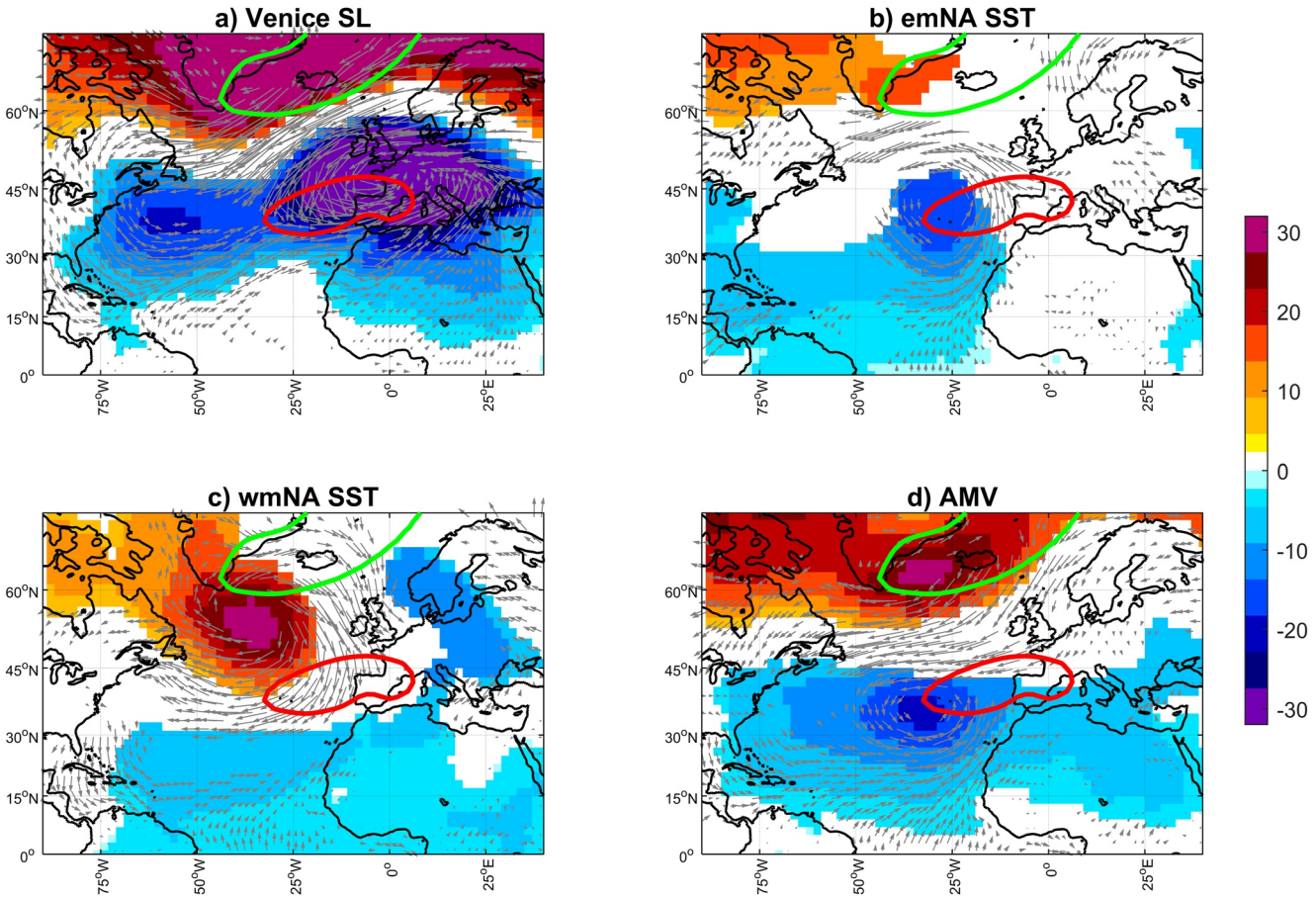

Figure 4. Atmospheric circulation anomalies associated to Venice sea-level (SL) and North Atlantic sea-surface temperature (SST) variability. Composite analysis of linearly detrended winter (October–March average) 1,000 hPa geopotential height (in meters) and 10 m wind (arrows) around positive (above the 75th percentile) and negative (below the 25th percentile) anomalies of linearly detrended measurements of (a) Venice SL (M_{VeSL}), (b) SST over the eastern midlatitude North Atlantic ($M_{emNASST}$), (c) SST over the western midlatitude North Atlantic ($M_{wmNASST}$), and (d) Atlantic multidecadal variability (AMV) (M_{AMV}). Shown are average values for positive minus negative values, where the composites test as significant at $p = 0.05$ based on the Mann-Whitney U test. The green and red line contours indicate 1,000 hPa geopotential height anomalies for composites around the NAO at 30 and −50 m, respectively.

R^2 value for the full-period (1873–2019) least squares regression linear trend (0.477). Most importantly, β_{VeSL} exhibits large multidecadal variations (Figure 5a), seen in the mean and envelope of its realizations, with decades of larger trends (e.g., around 1880–1890, around 1930 and since 2000) alternating with decades of smaller, even vanishing, trends (e.g., around the 1960s and 1970s). Such multidecadal variability in the trend is confirmed by the least squares estimates obtained via linear regressions on M_{VeSL} (Figure 2c), yielding, for instance, negative values for the period 1960–1989 (−1.29 mm/yr, [−1.57, −1.01]) and large positive values for the periods 1920–1949 (1.95 mm/yr, [1.21,2.69]) and 1990–2019 (4.05 mm/yr, [3.07,5.03]).

The evolution of β_{VeSL} superposes almost perfectly on that of β_{SPNASL} since the late 1940s (Figure 5a), when both local stochastic trend estimates indicate a slowdown of SL rise from around 0.11–0.12 cm/yr to around 0.06 cm/yr in the mid-1970s, followed by an acceleration to around 0.26 cm/yr in 2010. Before 1950, the evolutions diverge, with the largest differences found during 1910–1930 when β_{SPNASL} approaches zero while β_{VeSL} remains above values of 0.1 cm/yr. The transition from a distinct to a coherent SL rise pattern in Venice and the SPNA is evidenced by the difference $\delta_{Vesl} - \delta_{SPNASL}$: it rises between 1900 and 1930 to a maximum of about 3.6 cm, to then slowly stabilize around 2.8–3.2 cm since 1950 (Figure 2a). Therefore, since the mid-20th century the same processes likely governed SL rise in the SPNA and in Venice, but not before.

Recent SPNA SL evolution has been shown to closely depend on steric variations (Frederikse et al., 2020, see also Figure 5b). Estimates of the steric contribution to SPNA SL change are only available since the late 1950s and therefore do not cover the whole period of our analysis. Nevertheless, such dominance of the steric component

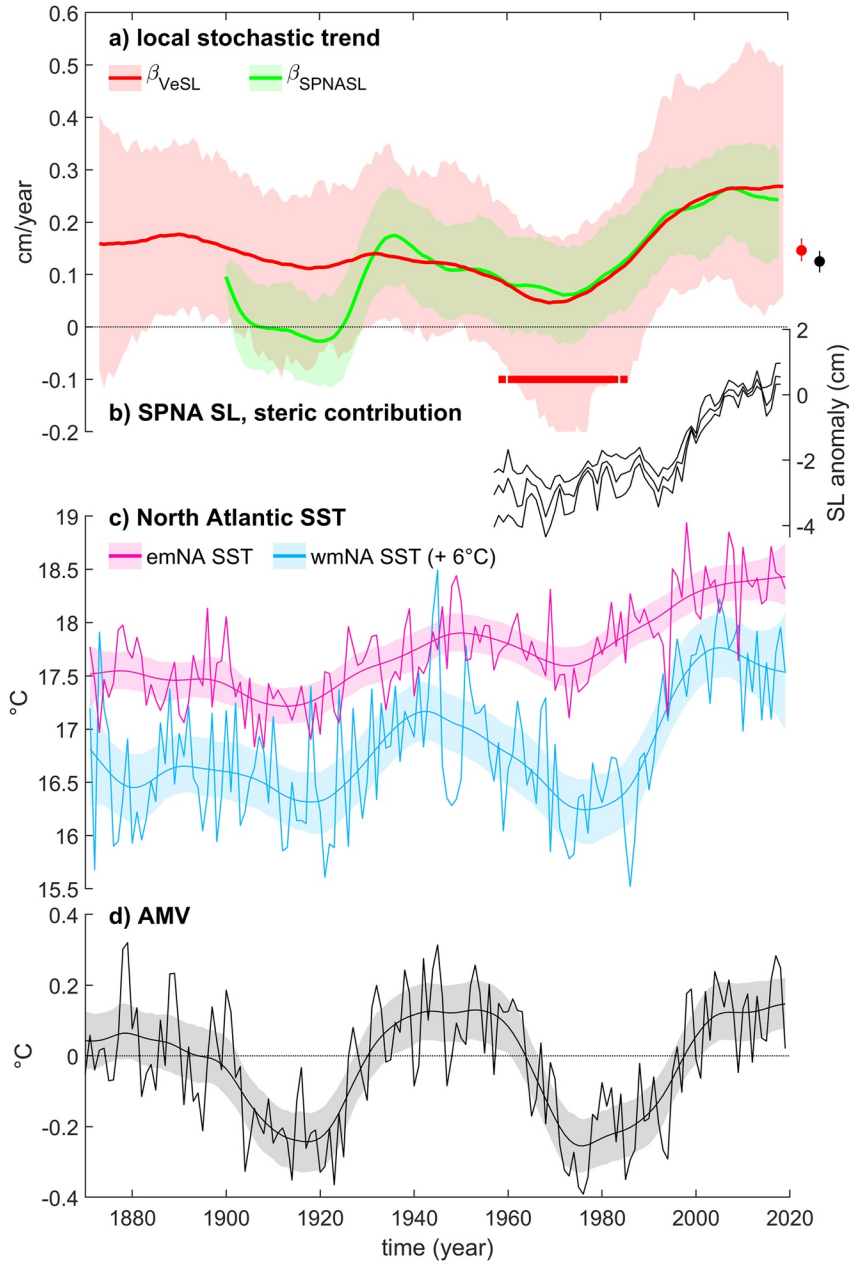

Figure 5. Evolution of sea-level (SL) trends and their connection with NA sea-surface temperature (SST). (a) Local stochastic trends β_{VeSL} (red) and β_{SPNASL} (green). The red bars at the bottom of the panel indicates when β_{VeSL} is not different from zero, that is, its 5–95 percentile range encompasses the value of zero. The circles and bars to the right of the panel indicate full-period (1873–2019) best estimates and associated uncertainty for β_{VeSL} (5–95 percentile range) and least square regression on M_{VeSL} (±2 standard error, see methods); (b) steric contribution to SPNA SL changes as estimated by Frederikse et al. (2020); (c) winter SST evolution for two key regions of the North Atlantic basin, namely the eastern midlatitude (emNA) and the western midlatitude North Atlantic (wmNA), as measurements and modeled states $\delta_{emNASST}$ and $\delta_{wmNASST}$; (d) winter AMV time series and associated modeled state δ_{AMV}. Illustration as for Figure 2.

since the mid-20th century could contribute to explain the onset of coherent SL trends in Venice and the SPNA. Accordingly, regression of winter North Atlantic SSTs on δ_{VeSL} demonstrates that Venice SL rise is associated with surface warming in the broad North Atlantic and Mediterranean basins, especially in the areas encompassing the Labrador Sea, the western subpolar gyre and the Gulf Stream regions, and the Levantine basin, but excluding the Gibraltar Strait area and its surroundings (Figure 3b). The regression pattern for δ_{VeSL} is more extensive than the one for δ_{SPNASL} (Figure 3e), but both patterns highlight the western portion of the midlatitude-to-subpolar

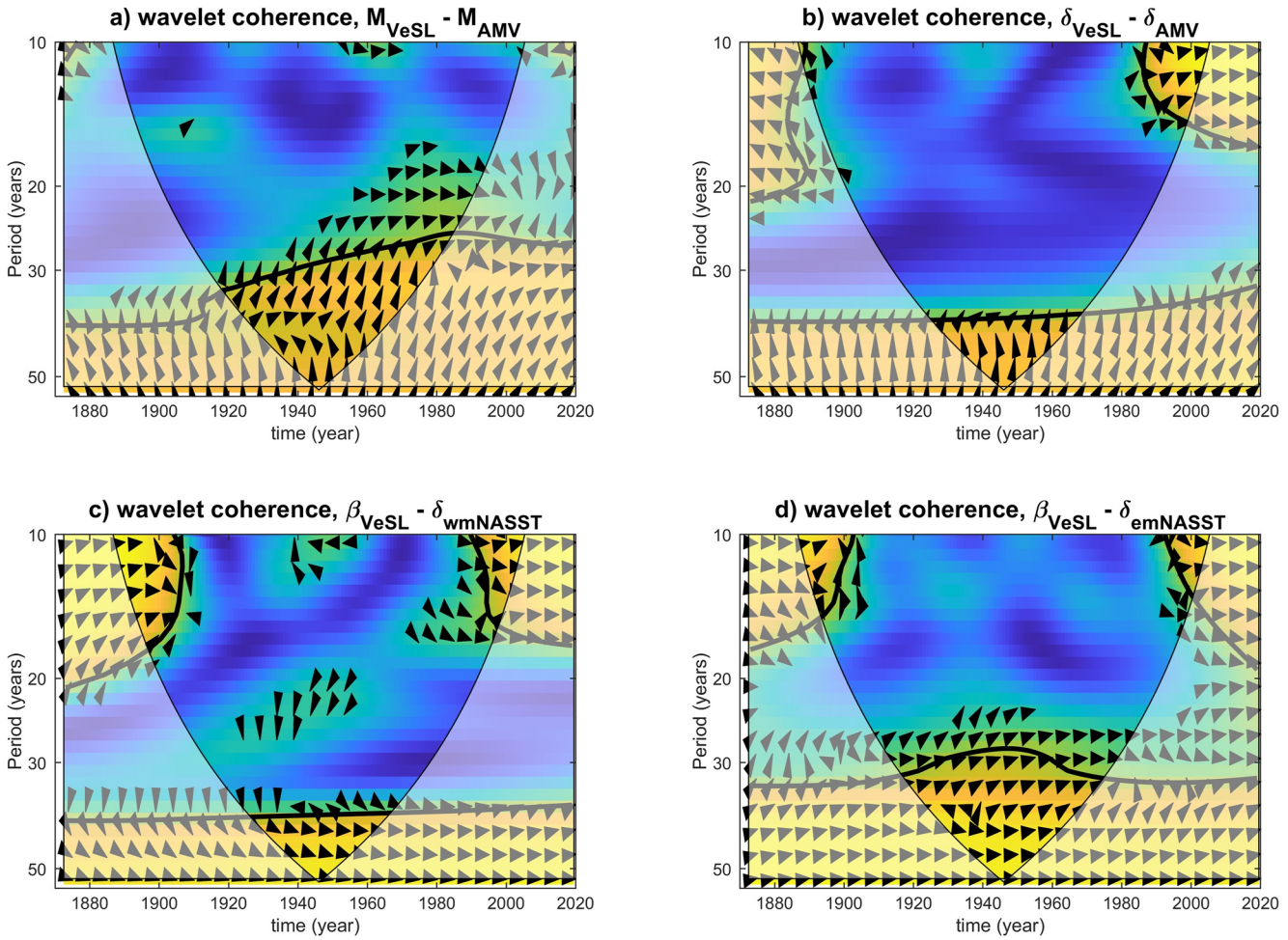

Figure 6. Wavelet coherence spectra between (a) measured time series of Venice sea-level (SL) (M_{VeSL}) and AMV (M_{AMV}), (b) the associated modeled states δ_{VeSL} and δ_{AMV}, and between the local stochastic trend for Venice SL (β_{VeSL}) and the modeled states δ of (c) sea-surface temperature (SST) over the western midlatitude North Atlantic, wmNA, and (d) the eastern midlatitude North Atlantic, emNA. Thick contours individuate regions of the time-frequency space where the coherence is statistically significant at 95% confidence; arrows indicate the phase difference; the cone of influence is reported as a thin line and light shading. All data are linearly detrended before analysis.

North Atlantic basin. When the analysis is restricted to the period 1950–2019 of coherent SL rise in Venice and the SPNA, the regression patterns for δ_{VeSL} and δ_{SPNASL} encompass also the eastern midlatitude North Atlantic and the whole Mediterranean Sea, including the Gibraltar Strait region (not shown). This supports the hypothesis that the tighter evolution of δ_{SPNASL} and δ_{VeSL} since the mid-20th century relates to the onset of a period when steric variations, seen as broad warming/cooling of the North Atlantic surface, predominate SPNA SL changes. The regression pattern of δ_{VeSL} overlaps well with the AMV pattern (Figure 3f), which describes basin-scale multidecadal variability of North Atlantic SST seen as alternating phases of broad warming and cooling anomalies. The wavelet coherence spectra calculated for both measured and modeled Venice SL and AMV (Figures 6a and 6b) confirm a significant connection around the 50-year periodicity, with Venice SL lagging the AMV by about 24 years.

Variations in the rate of local relative SL rise along the coasts of the Mediterranean Sea and in the North Atlantic Ocean in the proximity of the Gibraltar Strait (see locations in Figure 1b) are also coherent with the multidecadal fluctuations observed in the AMV (Table 2). Therefore, we interpret the AMV-Venice SL connection as follows: anomalous surface warming (cooling) of the subpolar and mid-latitude eastern North Atlantic during positive (negative) phases of the AMV forces steric SL variations in the North Atlantic ocean that propagate within the Mediterranean Sea through the Strait of Gibraltar (e.g., Adloff et al., 2018) and eventually affect Venice SL.

Table 2
Interdecadal Trends in Coastal Relative Sea-Level in the Eastern North Atlantic and in the Mediterranean Sea

	1905–1924 (AMV neg)	1935–1954 (AMV pos)	1970–1989 (AMV neg)	2000–2019 (AMV pos)
Cascais	−0.67, [−1.64 0.31] (204)	5.43, [3.89 6.97] (202)	2.07, [1.02 3.11] (234)	
Sines			1.08, [−1.93 4.09] (124)	4.92, [3.85 5.99] (223)
Marseille	1.32, [0.15 2.49] (240)	2.39, [0.69 4.09] (237)	0.04, [−1.16 1.24] (236)	3.45, [1.84 5.06] (206)
Genova		0.10, [−1.19 1.39] (237)	0.97, [−0.50 2.44] (195)	
Genova2				5.65, [3.50 7.81] (163)
Dubrovnik			0.39, [−0.96 1.74] (239)	3.04, [1.39 4.70] (224)
Split			0.08, [−1.34 1.51] (240)	1.51, [−0.24 3.27] (228)
Bakar			0.50, [−1.13 2.12] (240)	1.20, [−1.74 4.15] (168)

Note. Analysis is an ordinary least squares regression on monthly data for stations with PSMSL code (from top to bottom) 52, 1,456, 61, 59, 2,090, 760, 352, 353 over 20-year periods selected according to the state (positive or negative) of the AMV. Numbers are best estimate of trends (mm/yr) with 95% confidence intervals in brackets and number of data used in the analysis in parenthesis. At least 120 nonmissing data points are required for the analysis of a given period.

There is an evident extensive connection between β_{VeSL} and SST variations in the broad North Atlantic/Mediterranean area that strongly superpose on the AMV pattern (compare panels c and f in Figure 3). There is also an apparent connection between time series of β_{VeSL} and δ_{AMV} (Figures 5a and 5d). Furthermore, the wavelet coherence spectrum between β_{VeSL} and δ_{AMV} is significant at periods around 50 years, when β_{VeSL} leads δ_{AMV} by about 3–4 years (not shown). These results point to North Atlantic warm phases being associated with an acceleration of the local SL rise in Venice, and vice versa for cold AMV phases. Possibly, this represents an additional teleconnection between the North Atlantic climate and Venice SL changes, beyond the steric mechanism illustrated above. This possibility is supported by the existence of delayed oscillators in the coupled ocean-atmosphere in the North Atlantic identified in several modeling and observational studies (e.g., Bellucci et al., 2008; Li et al., 2013; Omrani et al., 2014; Omrani et al., 2022; Schneider et al., 2012; Sun et al., 2015; Zanchettin et al., 2019) and the spatiotemporal heterogeneity of basin-scale North Atlantic SST variability forced by the NAO (e.g., Sun et al., 2019, 2021; Zanchettin et al., 2014).

Accordingly, we explore atmospheric teleconnections linked to local SST anomalies in the North Atlantic over regions exhibiting a tighter connection between SST and β_{VeSL}. Two regions emerge from Figure 3c: the western midlatitude North Atlantic (wmNA) and the eastern midlatitude North Atlantic (emNA). Both regions display prominent multidecadal SST variability (Figure 5c). The wavelet coherence spectra between β_{VeSL}, and $\delta_{wmNASST}$ and $\delta_{emNASST}$ confirm a significant connection around the 50-year periodicity with small phase differences compatible with atmospheric teleconnection mechanisms (Figures 6c and 6d), specifically with $\delta_{wmNASST}$ lagging β_{VeSL} by about 4 years and $\delta_{emNASST}$ leading by about 1 year. The atmospheric circulation anomalies associated with warm emNA entail an anomalous low-pressure center around 30°–45°N and 25°–30°W that drives a cyclonic near-surface atmospheric circulation with an anomalous north-eastward flow along the North African western coast, which can contribute to generating SL anomalies in the approaches of the Strait of Gibraltar (Figure 4b) that can quickly propagate into the Mediterranean Sea yielding an acceleration of Venice SL. The anomalous atmospheric pattern for emNA does not superpose well on the NAO pattern but partly does so on the AMV pattern (Figure 4d), where the negative pressure anomaly in the approaches of the Strait of Gibraltar is less intense in the emNA compared to the AMV pattern but positioned more to the east. The wmNA pattern entails a positive pressure anomaly over the North Atlantic subpolar gyre region, west of 25°W and between 45°N and 60°N, with an associated strong anomalous anticyclonic circulation and northeasterly winds blowing over the UK and the Bay of Biscay (Figure 4c). This anticyclonic configuration partly superposes on the composite pattern of the mean sea-level pressure around major historical storm surges in Venice, especially before the peak of the events (Lionello, Nicholls, et al., 2021, their Figure 4). It might therefore be implicated in a multidecadal modulation of dynamics underlying Venice SL extremes.

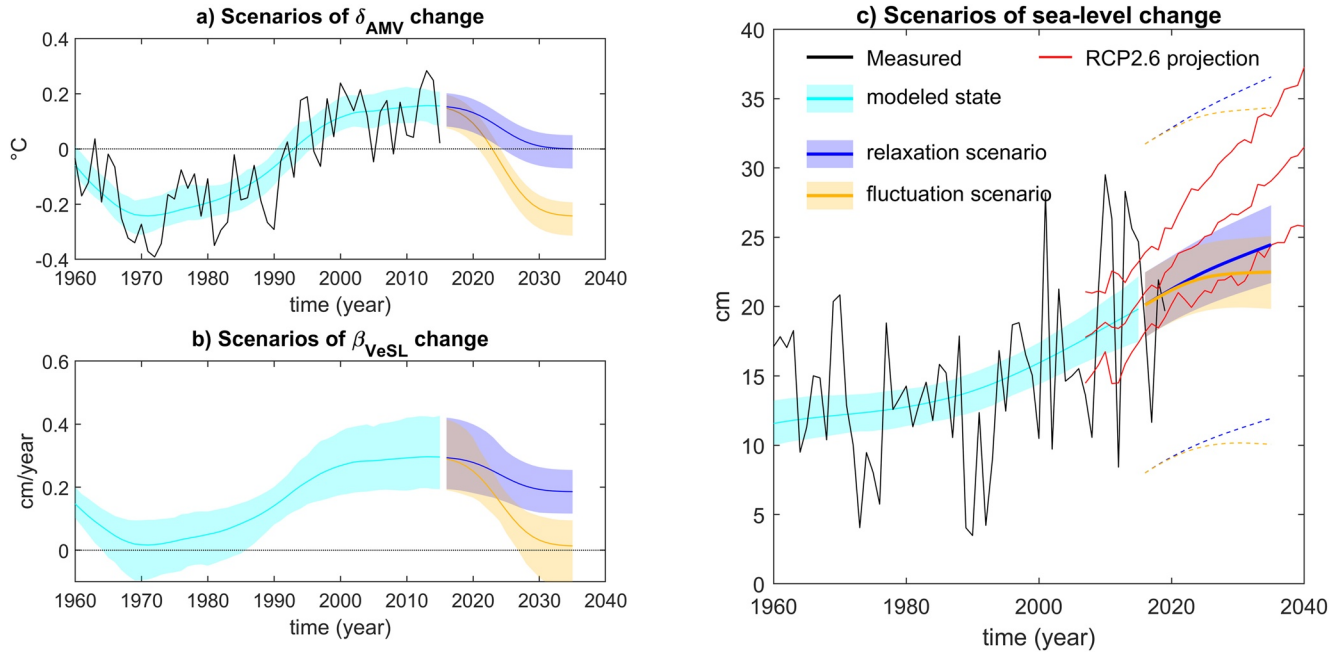

Figure 7. Scenarios of winter Venice SL rise to year 2035. (a) Idealized scenarios of future lagged AMV evolution: the relaxation scenario considers the AMV as a stochastic process whose values evolve toward zero; the fluctuation scenario considers the AMV as an oscillatory phenomenon and describes a transition to a negative phase comparable to historical variations. The AMV time series is lagged by −4 years; (b) evolution of the local stochastic trend of winter Venetian MSL conditioned to the lagged AMV historical evolution and scenarios. (c) The two future scenarios of winter Venice SL in the context of historical observations. The red lines illustrate the 5–95 percentile range and the mean for projection of Venice SL under the RCP2.6 anthropogenic greenhouse gas emission scenario from Zanchettin et al. (2021a). Lines are mean of realizations and shading is the associated 5–95 percentile range. The dashed lines in (c) describe the range of variations accounting for observational uncertainty and encompassing interannual variability.

4. Implications for Near-Term Predictability

The existence of substantial multidecadal variations in historical SL observations in Venice, the Mediterranean Sea and the subpolar and midlatitude eastern North Atlantic that superpose on the long-term centennial trend and contribute to periodic strengthening and weakening of SL rise motivates a strengthened focus on near-term SL predictability and prediction in these regions. Also, oceanic observations and theoretical arguments indicate the possibility of a switch in the next decades to a sustained negative phase of the AMV comparable to the one occurred in the 1960s–1970s (Frajka-Williams et al., 2017; Omrani et al., 2022). Otherwise, if the AMV is seen as a manifestation of stochastic variability (e.g., Mann et al., 2020), it shall revert to a neutral phase sooner or later. To illustrate the potential effects of such AMV cooling on Venice SL we build two idealized scenarios of AMV evolution to the year 2035 (see Section 2). The first entails the onset of a negative phase comparable, in magnitude, to the previous one and is referred to as "fluctuation scenario"; the second describes a transition to a neutral value and is referred to as "relaxation scenario" (Figure 7a). The AMV data are lagged by −4 years to reflect the wavelet phasing between AMV and Venice SL trend.

We linearly regress between realizations of β_{VeSL} on lagged δ_{AMV} for the period since 1960 and retain models with associated R^2 above 0.9. The so-obtained pool of regression models is used to estimate β_{VeSL} for the period 2020–2035 under the hypotheses of AMV forcing and persistent tight coupling between North Atlantic and Venice SL variations as found since the mid-20th century. Then, δ_{VeSL} and M_{VeSL} are calculated based on Equations 1–3 using noise estimates obtained from the historical period. To illustrate the potential for decadal predictions to provide an added value with respect to long-term projections, we consider the RCP2.6 scenario for Venice SL illustrated in Zanchettin et al., 2021a. We adapt the original values for the annual Venice SL to the winter Venice SL by calculating anomalies as departures from the average of δ_{VeSL} for the 2007–2019 period when observational and scenario data overlap. Both AMV scenarios yield a reduction of β_{VeSL}, which settles around values of 0.2 cm/yr for the relaxation scenario, and around zero for the fluctuation scenario (Figure 7b). As a result, the δ_{VeSL} evolution conditioned by the AMV scenarios substantially deviates from the long-term projection

in the next decades, especially in the case of the stronger AMV fluctuation scenario, for which a decadal hiatus in the Venice SL rise can be identified. Therefore, unless the AMV persists in a strong positive phase, according to our regression model the rise of Venice SL is expected to slow down in the next one-and-half decade compared to what has been observed since the beginning of the 21st century. Of course, the proposed scenarios are not formal predictions despite they build on physical arguments and include some level of realism; so, they do not constrain, year after year, the range of future evolutions of winter Venice SL. The fluctuation scenario, which describes an imminent AMV transition toward persistent negative values, can be considered as a bottom-end scenario, where duration and magnitude of the slowdown are maximized. Inclusion of observational uncertainty, which is dominated by interannual variability, renders our scenarios for M_{VeSL} much less constrained than for δ_{VeSL}. This demonstrates the need to improve understanding of the connection between interannual Venice SL variations and their large-scale predictors, particularly the NAO, and explore their predictability. Finally, in terms of impact it is the relative SL that matters, and linear extrapolation of current subsidence estimates could provide additional ∼6 mm to ∼6 cm rise of the relative SL in Venice in 2035 compared to the present.

5. Conclusions and Outlook

This study reveals significant multidecadal trend variations in winter Venice sea level linked to large-scale multidecadal oceanic and atmospheric variability in the North Atlantic sector linked with the AMV. The employed methodology based on Bayesian hierarchical models allows to overcome limitations related to a lack of information about uncertainty related to the various processes contributing to historical local sea-level variability, most noticeably subsidence, whose explicit treatment remains a gap to be filled by follow up studies. This study also provides a first attempt toward near-term prediction of Venice sea level based on idealized scenarios that build on an intrinsic feature of the AMV, that is, that its associated anomalies will sooner or later dampen and possibly change sign, and that the related index will hence revert to neutral or even negative values. Results indicate that this will correspond to a temporary slowdown in Venetian relative sea-level rise, which may even shape as a decadal hiatus. Given the tight agreement of sea-level variability on a broad band of timescales along the northern Adriatic coast and also, as shown here, more generally the Mediterranean Sea, these results may be relevant beyond the local case of Venice. Apart the scientific implications of this findings, we believe that proper communication of this variability is crucial for management and protection activities of this world-class historical site, as well as for increasing the public awareness and preparedness on the potentially significant implications of natural climate variability for the mid-term future evolution of regional and local climates. In this sense, this first attempt of ours to explore the potential predictability of sea-level change in Venice in the upcoming couple of decades should be seen as aimed at fostering better acknowledgment of the role of natural climate variability for transient climate evolution and improved communication of the associated uncertainty, especially of its potential for temporary yet significant deviations from the expected forced response under scenarios of increasing greenhouse gas concentrations.

Data Availability Statement

Relevant data used in this study can be obtained at https://doi.org/10.5281/zenodo.7059739 (Zanchettin, 2022).

Acknowledgments
D. Z. conceived the study, performed the analyses and drafted the manuscript. S. R. and A. R. contributed to discussion and finalization of the paper. The statistical model is developed in Matlab using the dlmsmo routine by Marko Laine (http://helios.fmi.fi/~lainema/dlm/). Maps are plotted with the m_map package (Pawlowicz, 2000) for MATLAB software. Scientific activity was performed in the Research Programme Venezia2021, with the contribution of the Provveditorato for the Public Works of Veneto, Trentino Alto Adige and Friuli Venezia Giulia, provided through the concessionary of State Consorzio Venezia Nuova and coordinated by CORILA. The authors thank Sara Bruni for the fruitful discussions on subsidence estimates for Venice and satellite altimetry datasets.

References

Adloff, F., Jordà, G., Somot, S., Sevault, F., Meyssignac, B., Arsouze, T., et al. (2018). Improving sea level simulation in Mediterranean regional climate models. *Climate Dynamics*, *51*, 1167–1178. https://doi.org/10.1007/s00382-017-3842-3

Andrews, D. W. K., & Monohan, J. C. (1992). An improved heteroskedasticity and autocorrelation consistent covariance matrix estimator. *Econometrica*, *60*, 953–966. https://doi.org/10.2307/2951574

Arisido, M. W., Gaetan, C., Zanchettin, D., & Rubino, A. (2017). A Bayesian hierarchical approach for spatial analysis of climate model bias in multi-model ensembles. *Stochastic Environmental Research and Risk Assessment*, *31*, 2645–2657. https://doi.org/10.1007/s00477-017-1383-2

Battistin, D., & Canestrelli, P. (2006). *La serie Storica Delle maree a Venezia: 1872–2004 (the time series of Venetian tides: 1872– 2004)* (p. 210). Venice, Italy: Ist. Centro Segnalazioni e Previsioni Maree. Retrieved from https://www.comune.venezia.it/content/download-pubblicazioni

Bednar-Friedl, B., Biesbroek, R., Schmidt, D. N., Alexander, P., Børsheim, K. Y., Carnicer, J., et al. (2022). Europe. In H.-O. Pörtner, D. C. Roberts, M. Tignor, E. S. Poloczanska, K. Mintenbeck, A. Alegría, et al. (Eds.), *Climate change 2022: Impacts, adaptation, and vulnerability*. In *Contribution of working group II to the sixth assessment report of the intergovernmental panel on climate change* (pp. 1817–1927). Cambridge University Press. https://doi.org/10.1017/9781009325844.015

Bellucci, A., Gualdi, S., Scoccimarro, E., & Navarra, A. (2008). NAO-ocean circulation interactions in a coupled general circulation model. *Climate Dynamics*, *31*, 759–777. https://doi.org/10.1007/s00382-008-0408-4

Bruni, S., Fenoglio, L., Raicich, F., & Zerbini, S. (2022). On the consistency of coastal sea-level measurements in the Mediterranean Sea from tide gauges and satellite radar altimetry. *Journal of Geodesy*, *96*, 41. https://doi.org/10.1007/s00190-022-01626-9

Buser, C. M., Künsch, H. R., Lüthi, D., Wild, M., & Schär, C. (2009). Bayesian multi-model projection of climate: Bias assumptions and interannual variability. *Climate Dynamics*, *33*, 849–868. https://doi.org/10.1007/s00382-009-0588-6

Canargo, C. M. L., Riva, R. E. M., Hermans, T. H. J., & Slangen, A. B. A. (2021). Trends and uncertainties of regional barystatic sea-level change in the satellite altimetry era. [preprint, accepted for publication]. Earth System Dynamics Discussion. https://doi.org/10.5194/esd-2021-80

Cavaleri, L., Bajo, M., Barbariol, F., Bastianini, M., Benetazzo, A., Bertotti, L., et al. (2020). The 2019 flooding of Venice and its implications for future predictions. *Oceanography*, *33*(1), 42–49. https://doi.org/10.5670/oceanog.2020.105

Cazenave, A., & Nerem, R. S. (2004). Present-day sea level change: Observations and causes. *Reviews of Geophysics*, *42*, RG3001. https://doi.org/10.1029/2003RG000139

Chafik, L., Nilsen, J. E. Ø., Dangendorf, S., Reverdin, G., & Frederikse, T. (2019). North Atlantic ocean circulation and decadal sea level change during the altimetry era. *Scientific Reports*, *9*, 1041. https://doi.org/10.1038/s41598-018-37603-6

Chambers, D. P., Merrifield, M. A., & Nerem, R. S. (2012). Is there a 60-year oscillation in global mean sea level? *Geophysical Research Letters*, *39*, L18607. https://doi.org/10.1029/2012GL052885

Church, J. A., Clark, P. U., Cazenave, A., Gregory, J. M., Jevrejeva, S., Levermann, A., et al. (2013). Sea level change. In T. F. Stocker, D. Qin, G.-K. Plattner, M. Tignor, S. K. Allen, J. Boschung, et al. (Eds.), *Climate change 2013: The physical science basis*. In *Contribution of working group I to the Fifth assessment report of the intergovernmental panel on climate change*. Cambridge University Press.

Compo, G. P., Whitaker, J. S., Sardeshmukh, P. D., Matsui, N., Allan, R. J., & Yin, X. (2011). The twentieth century reanalysis Project. *The Quarterly Journal of the Royal Meteorological Society*, *137*, 1–28. https://doi.org/10.1002/qj.776

Dangendorf, S., Macros, M., Wöppelmann, G., Conrad, C. P., Frederikse, T., Riva, R., et al. (2017). Reassessment of 20th century global mean sea level rise. *Proceedings of the National Academy of Sciences of the United States of America*, *114*, 5946–5951. https://doi.org/10.1073/pnas.1616007114

Duan, Q., & Phillips, T. J. (2010). Bayesian estimation of local signal and noise in multimodel simulations of climate change. *Journal of Geophysical Research*, *115*, D18123. https://doi.org/10.1029/2009JD013654

Enfield, D. B., Mestas-Nuñez, A. M., & Trimble, P. J. (2001). The Atlantic multidecadal oscillation and its relation to rainfall and river flows in the continental US. *Geophysical Research Letters*, *28*, 2077–2080. https://doi.org/10.1029/2000GL012745

Ferrarin, C., Bajo, M., Benetazzo, A., Cavaleri, L., Chiggiato, J., Davison, S., et al. (2021). Local and large-scale controls of the exceptional Venice floods of November 2019. *Progress in Oceanography*, *197*, 102628. https://doi.org/10.1016/j.pocean.2021.102628

Fox-Kemper, B. T., Hewitt, H., Xiao, C., Aðalgeirsdóttir, G., Drijfhout, S. S., & Edwards, T. L. (2021). Climate Change 2021: The physical science basis. In Masson, V. Delmotte, P.Zhai, A. Pirani, S. L. Connors, & C. S. Péan (Eds.), *Contribution of working group I to the sixth assessment report of the intergovernmental panel on climate change*. Cambridge University Press.

Frajka-Williams, E., Beaulieu, C., & Duchez, A. (2017). Emerging negative Atlantic Multidecadal Oscillation index in spite of warm subtropics. *Scientific Reports*, *7*, 11224. https://doi.org/10.1038/s41598-017-11046-x

Frederikse, T., Landerer, F., Caron, L., Adhikari, S., Parkes, D., Humphrey, V. W., et al. (2020). The causes of sea-level rise since 1900. *Nature*, *584*(7821), 393–397. https://doi.org/10.1038/s41586-020-2591-3

Galassi, G., & Spada, G. (2014). Linear and non-linear sea-level variations in the Adriatic Sea from tide gauge records (1872–2012). *Annals of Geophysics*, *57*(6). https://doi.org/10.4401/ag-6536

Gregory, J. M., Griffies, S. M., Hughes, C. W., Lowe, J. A., Church, J. A., Fukimori, I., et al. (2019). Concepts and terminology for Sea Level: Mean, variability and change, both local and global. *Surveys in Geophysics*, *40*(6), 1251–1289. https://doi.org/10.1007/s10712-019-09525-z

Grinsted, A., Moore, J. C., & Jevrejeva, S. (2004). Application of the cross wavelet transform and wavelet coherence to geophysical time series. *Nonlinear Processes in Geophysics*, *11*, 561–566. https://doi.org/10.5194/npg-11-561-2004

Hay, C. C., Morrow, E., Kopp, R. E., & Mitrovica, J. X. (2015). Probabilistic reanalysis of twentieth-century sea-level rise. *Nature*, *517*, 481–484. https://doi.org/10.1038/nature14093

Holgate, S. J., Matthews, A., Woodworth, P. L., Rickards, L. J., Tamisiea, M. E., Bradshaw, E., et al. (2013). New data systems and products at the permanent Service for mean sea level. *Journal of Coastal Research*, *29*(3), 493–504. https://doi.org/10.2112/JCOASTRES-D-12-00175.1

Jones, P. D., Jónsson, T., & Wheeler, D. (1997). Extension to the North Atlantic Oscillation using early instrumental pressure observations from Gibraltar and South-West Iceland. *International Journal of Climatology*, *17*, 1433–1450. https://doi.org/10.1002/(sici)1097-0088(19971115)17:13<1433::aid-joc203>3.0.co;2-p.CO;2

Kang, E. L., Cressie, N., & Sain, S. R. (2012). Combining outputs from the north American regional climate change assessment program by using a Bayesian hierarchical model. *Journal of the Royal Statistical Society: Series C*, *61*, 291–313. https://doi.org/10.1111/j.1467-9876.2011.01010.x

Kopp, R. E., Horton, R. M., Little, C. M., Mitrovica, J. X., Oppenheimer, M., Rasmussen, D. J., et al. (2014). Probabilistic 21st and 22nd century sea level projections at a global network of tide-gauge sites. *Earth's Future*, *2*, 383–406. https://doi.org/10.1002/2014EF000239

Laine, M., Latva-Pukkila, N., & Kyrölä, E. (2014). Analysing time-varying trends in stratospheric ozone time series using the state space approach. *Atmospheric Chemistry and Physics*, *14*, 9707–9725. https://doi.org/10.5194/acp-14-9707-2014

Latif, M., Sun, J., Visbeck, M., & Bordbar, H. (2022). Natural variability has dominated Atlantic meridional overturning circulation since 1900. *Nature Climate Change*, *12*, 455–460. https://doi.org/10.1038/s41558-022-01342-4

Li, J., Sun, C., & Jin, F. F. (2013). NAO implicated as a predictor of Northern Hemisphere mean temperature multidecadal variability. *Geophysical Research Letters*, *40*, 5497–5502. https://doi.org/10.1002/2013GL057877

Lionello, P., Barriopedro, D., Ferrarin, C., Nicholls, R. J., Orlic, M., Raicich, F., et al. (2021). Extreme floods of Venice: Characteristics, dynamics, past and future evolution (review article). *Natural Hazards and Earth System Sciences*, *21*, 2705–2731. https://doi.org/10.5194/nhess-21-2705-2021

Lionello, P., Nicholls, R. J., Umgiesser, G., & Zanchettin, D. (2021). Venice flooding and sea level: Past evolution, present issues, and future projections (introduction to the special issue). *Natural Hazards and Earth System Sciences*, *21*, 2633–2641. https://doi.org/10.5194/nhess-21-2633-2021

Mann, M. E., Steinman, B. A., & Miller, S. K. (2020). Absence of internal multidecadal and interdecadal oscillations in climate model simulations. *Nature Communications*, *11*, 49. https://doi.org/10.1038/s41467-019-13823-w

Meli, M., & Romagnoli, C. (2022). Evidence and implications of hydrological and climatic change in the Reno and Lamone river basins and related coastal areas (Emilia-Romagna, northern Italy) over the last century. *Water*, *14*, 2650. https://doi.org/10.3390/w14172650

Omrani, N. E., Bader, J., Keenlyside, N. S., & Manzini, E. (2014). Troposphere-stratosphere response to large-scale North Atlantic Ocean variability in an atmosphere/ocean coupled model. *Climate Dynamics*, *46*, 1397–1415. https://doi.org/10.1007/s00382-015-2654-6

Omrani, N.-E., Keenlyside, N., Matthes, K., Boljka, L., Zanchettin, D., Jungclaus, J. H., & Lubis, S. W. (2022). Coupled stratosphere-troposphere-Atlantic multidecadal oscillation and its importance for near-future climate projection. *NPJ Climate and Atmospheric Science*, *5*, 59. https://doi.org/10.1038/s41612-022-00275-1

Oppenheimer, M., & Glavovic, B. (2019). Sea level rise and implications for low Lying Islands, coasts and communities. In *IPCC special report on the ocean and cryosphere in a changing climate* (pp. 321–445). Cambridge University Press.

Pawlowicz, R. (2000). *M_Map: A mapping package for Matlab*. University of British. Columbia Earth and Ocean Sciences [Online]. Retrieved from http://www.eos.ubc.ca/rich/map.html

Permanent service for mean sea level. (2022). *Tide gauge data*. PSMSL. Retrieved from http://www.psmsl.org/data/obtaining/

Radford, N. M. (2003). Slice sampling. *Annals of Statistics*, *31*, 705–767.

Rayner, N. A., Parker, D. E., Horton, E. B., Folland, C. K., Alexander, L. V., Rowell, D. P., et al. (2003). Global analyses of sea surface temperature, sea ice, and night marine air temperature since the late nineteenth century. *Journal of Geophysical Research*, *108*(D14), 4407. https://doi.org/10.1029/2002JD002670

Rovere, A., Stocchi, P., & Vacchi, M. (2016). Eustatic and relative sea level changes. *Current Climate Change Reports*, *2*, 221–231. https://doi.org/10.1007/s40641-016-0045-7

Scafetta, N. (2014). Multi-scale dynamical analysis (MSDA) of sea level records versus PDO, AMO, and NAO indexes. *Climate Dynamics*, *43*, 175–192. https://doi.org/10.1007/s00382-013-1771-3

Schneider, E. K., & Fan, M. (2012). Observed decadal North Atlantic tripole SST variability. Part II: Diagnosis of mechanisms. *Journal of Climate*, *69*, 51–64. https://doi.org/10.1175/jas-d-11-019.1

Slangen, A. B. A., Carson, M., Katsman, C. A., vande Wal, R. S. W., Köhl, A., Vermeersen, L. L. A., & Stammer, D. (2014). Projecting twenty-first century regional sea-level changes. *Climatic Change*, *124*, 317–332. https://doi.org/10.1007/s10584-014-1080-9

Slangen, A. B. A., Church, J. A., Agosta, C., Fettweis, X., Marzeion, B., & Richter, K. (2016). Anthropogenic forcing dominates global mean sea-level rise since 1970. *Nature Climate Change*, *6*, 701–705. https://doi.org/10.1038/nclimate2991

Smith, D. M., Scaife, A. A., Eade, R., Athanasiadis, P., Bellucci, A., Bethke, I., et al. (2020). North Atlantic climate far more predictable than models imply. *Nature*, *583*, 796–800. https://doi.org/10.1038/s41586-020-2525-0

Sun, C., Li, J., & Jin, F. F. (2015). A delayed oscillator model for the quasi-periodic multidecadal variability of the NAO. *Climate Dynamics*, *45*(7), 2083–2099. https://doi.org/10.1007/s00382-014-2459-z

Sun, C., Li, J., Kucharski, F., Xue, J., & Li, X. (2019). Contrasting spatial structures of Atlantic Multidecadal Oscillation between observations and slab ocean model simulations. *Climate Dynamics*, *52*(3), 1395–1411. https://doi.org/10.1007/s00382-018-4201-8

Sun, C., Zhang, J., Li, X., Shi, C., Gong, Z., Ding, R., et al. (2021). Atlantic meridional overturning circulation reconstructions and instrumentally observed multidecadal climate variability: A comparison of indicators. *International Journal of Climatology*, *41*(1), 763–778. https://doi.org/10.1002/joc.6695

Tebaldi, C., Smith, R. L., Nychka, D., & Mearns, L. O. (2005). Quantifying uncertainty in projections of regional climate change: A Bayesian approach to the analysis of multimodel ensembles. *Journal of Climate*, *18*, 1524–1540. https://doi.org/10.1175/jcli3363.1

Thiéblemont, R., Le Cozannet, G., Toimil, A., Meyssignac, B., & Losada, I. J. (2019). Likely and high-end impacts of regional sea-level rise on the Shoreline change of European Sandy coasts under a high greenhouse gas emissions scenario. *Water*, *11*(12), 2607. https://doi.org/10.3390/w11122607

Torrence, C., & Webster, P. W. (1999). Interdecadal changes in the ENSO-monsoon system. *Journal of Climate*, *12*, 2679–2690. https://doi.org/10.1175/1520-0442(1999)012<2679:ICITEM>2.0.CO;2

Tosi, L., Lio, C. D., Teatini, P., & Strozzi, T. (2018). Land subsidence in coastal environments: Knowledge advance in the Venice Coastland by TerraSAR-X PSI. *Remote Sensing*, *10*, 1191. https://doi.org/10.3390/rs10081191

Tosi, L., Teatini, P., & Strozzi, T. (2013). Natural versus anthropogenic subsidence of Venice. *Scientific Reports*, *3*, 2710. https://doi.org/10.1038/srep02710

Umgiesser, G. (2020). The impact of operating the mobile barriers in Venice (MOSE) under climate change. *Journal of Nature Conservation*, *54*, 125783. https://doi.org/10.1016/j.jnc.2019.125783

Umgiesser, G., Bajo, M., Ferrarin, C., & Cucco, A. (2021). The prediction of floods in Venice: Methods, models and uncertainty (review article). *Natural Hazards and Earth System Sciences*, *21*, 2679–2704. https://doi.org/10.5194/nhess-21-2679-2021

Vecchio, A., Anzidei, M., Serpelloni, E., & Florindo, F. (2019). Natural variability and vertical land motion contributions in the Mediterranean sea-level records over the last two centuries and projections for 2100. *Water*, *11*, 1480. https://doi.org/10.3390/w11071480

Zanchettin, D. (2022). Data from article "Is the Atlantic a Source for Decadal Predictability of Sea-Level Rise in Venice?". Zenodo. [Dataset]. https://doi.org/10.5281/zenodo.7059739

Zanchettin, D., Bothe, O., Müller, W., Bader, J., & Jungclaus, J. H. (2014). Different flavors of the Atlantic multidecadal variability. *Climate Dynamics*, *42*, 381–399. https://doi.org/10.1007/s00382-013-1669-0

Zanchettin, D., Bruni, S., Raicich, F., Lionello, P., Adloff, F., Androsov, A., et al. (2021a). sea-Level rise in Venice: Historic and future trends (review article). *Natural Hazards and Earth System Sciences*, *21*, 2643–2678. https://doi.org/10.5194/nhess-21-2643-2021

Zanchettin, D., Bruni, S., Thiéblemont, R., & Rubinetti, S. (2021b). Data from article "Sea-level rise in Venice: Historic and future trends (review article)". Zenodo. [Dataset]. https://doi.org/10.5281/zenodo.5139890

Zanchettin, D., Rubino, A., Traverso, P., & Tomasino, M., (2009). Teleconnections force interannual-to-decadal tidal variability in the Lagoon of Venice (northern Adriatic). *Journal of Geophysical Research*, *114*, D07106. https://doi.org/10.1029/2008JD011485

Zanchettin, D., Toniazzo, T., Taricco, C., Rubinetti, S., Rubino, A., & Tartaglione, N. (2019). Atlantic origin of asynchronous European interdecadal hydroclimate variability. *Scientific Reports*, *9*, 10998. https://doi.org/10.1038/s41598-019-47428-6

Zanchettin, D., Traverso, P., & Tomasino, M. (2006). Discussion on sea level fluctuations along the Adriatic coasts coupling to climate indices forced by solar activity: Insights into the future of Venice. *Global Planetary Change*, *50*, 226–234. https://doi.org/10.1016/j.gloplacha.2006.01.001

Zerbini, S., Raicich, F., Prati, C. M., Bruni, S., Del Conte, S., Errico, M., & Santi, E. (2017). Sea level change in the Northern Mediterranean Sea from long-period tide gauge time series. *Earth-Science Reviews*, *167*, 72–87. https://doi.org/10.1016/j.earscirev.2017.02.009